Oncogene (2007) 26, 425–440

www.nature.com/onc

ORIGINAL ARTICLE

Annexin II binds progastrin and gastrin-like peptides, and mediates growth factor effects of autocrine and exogenous gastrins on colon cancer and intestinal epithelial cells

P Singh[1], H Wu[1], C Clark[2] and A Owlia[1]

[1]*Department of Neuroscience and Cell Biology, University of Texas Medical Branch, Galveston, TX, USA and* [2]*Ciphergen Biosystems, Inc., Fremont, CA, USA*

We and others have reported the presence of novel progastrin (PG)/gastrin receptors on normal and cancerous intestinal cells. We had earlier reported the presence of 33–36 kDa gastrin-binding proteins on cellular membranes of colon cancer cells. The goal of the current study was to identify the protein(s) in the 33–36 kDa band, and analyse its functional significance. A carbodiimide crosslinker was used for crosslinking radio-labeled gastrins to membrane proteins from gastrin/PG responsive cell lines. Native membrane proteins, crosslinked to the ligand, were solubulized and enriched by >1000-fold, and analysed by surface-enhanced laser desorption/ionization-time of flight-mass spectrometry. The peptide masses were researched against the NCBInr database using the ProFound search engine. Annexin II (ANX II) was identified, and confirmed by matrix-assisted laser desorption/ionization-time of flight-mass spectrometry. As HCT-116 cells express autocrine PG, the *in situ* association of PG with ANX II was demonstrated in pulldown assays. Direct binding of PG with ANX II was confirmed in an *in vitro* binding assay. In order to confirm a functional importance of these observations, sense and anti-sense (AS) ANX II RNA-expressing clones of intestinal epithelial (IEC-18) and human colon cancer (HCT-116) cell lines were generated. AS clones demonstrated a significant loss in the growth response to exogenous (IEC-18) and autocrine (HCT-116) PG. We have thus discovered that membrane-associated ANX II binds PG/gastrins, and partially mediates growth factor effects of the peptides.
Oncogene (2007) **26,** 425–440. doi:10.1038/sj.onc.1209798; published online 10 July 2006

Keywords: M_r of gastrin-binding proteins; SELDI-TOF-MS; antisense and sense Annexin II RNA

Correspondence: Professor P Singh, Department of Neuroscience and Cell Biology, 10.104 Medical Research Building, Route 1043, University of Texas Medical Branch, Galveston, TX 77555-1043, USA.
E-mail: posingh@utmb.edu
Received 22 March 2006; revised 2 May 2006; accepted 25 May 2006; published online 10 July 2006

Introduction

Progastrin and gastrin peptides are expressed in neuroendocrine cells in the brain and antral part of the stomachs and processed into the precursor peptide (PG) and glycine extended form of gastrins (GG); subsequent amidation at the C-terminal end generates amidated forms of gastrins (G17, G34) (Dockray *et al*., 1996). Under physiological conditions, only processed forms of gastrins (G17, G34) are present as the major circulating forms of gastrins (Dockray *et al*., 1996).

PG, GG and G17 exert proliferative effects on normal and cancerous gastrointestinal (GI) cells *in vitro* and *in vivo* (Wang *et al*., 1996; Hollande *et al*., 1997; Koh *et al*., 1999; Baldwin *et al*., 2001; Brown *et al*., 2003; Singh *et al*., 2003; Ottewell *et al*., 2005). PG and GG exert co-carcinogenic effects on colon carcinogenesis in response to azoxymethane (Singh *et al*., 2000a, b; Aly *et al*., 2001; Cobb *et al*., 2004). Elevated levels of circulating PG are measured in hypergastrinemia owing to various etiologies (including ZE syndrome and pernicious anemia) (Rengifo-Cam and Singh, 2004), and in patients with colorectal cancer (CRC) (Siddheshwar *et al*., 2001). As potent co-carcinogenic effects of PG are reported in Fabp-PG mice, that express 'patho-physiological' concentrations of hPG (0.1–5 nM) (Cobb *et al*., 2004), it suggests that elevated levels of circulating PG, as measured in patients with hyperastrinemia and CRC, may play a role in colon carcinogenesis.

Besides circulating gastrins, autocrine gastrins (mainly PG), play an equally important role in maintaining growth and tumorigenic potential of gastrin-dependent tumors (Singh *et al*., 1996; Hollande *et al*., 1997; Rengifo-Cam and Singh, 2004). Recent studies further highlight an important role of colon cancer-associated oncogenic pathways (mutant Ras and Wnt/β-catenin) in upregulating the gastrin gene expression in CRCs (Lei *et al*., 2004; Chakladar *et al*., 2005).

We now know that increased proliferation and decreased apoptosis contributes to the growth factor and co-carcinogenic effects of PG-like peptides (Wu *et al*., 2000, 2003; Singh *et al*., 2003; Rengifo-Cam and Singh, 2004). Several receptor (R)-subtypes bind gastrin and choecystokinin octapeptide (CCK)-like peptides. Cholecystokinin type 1 receptor (CCK_1R) mainly bind

CCK-like peptides and have negligible affinity for gastrins (Kopin *et al*., 1992; Wank *et al*., 1992). Cholecystokinin type 2 receptor (CCK_2R) bind amidated gastrins and CCK with almost equal affinity, but demonstrate negligible affinity for non-amidated gastrins (Kopin *et al*., 1992). Low-affinity gastrin-binding sites ($K_d = \sim 1.0\,\mu M$) termed CCKC-R bind PG and gastrins (Zhang and Baldwin, 1994). High-affinity binding sites (receptors?) were identified that were distinct from CCK_1R, CCK_2R and CCKC-R (Chicone *et al*., 1989; Narayan *et al*., 1992; Seva *et al*., 1994; Singh *et al*., 1995, 2003; Baldwin *et al*., 2001). These novel binding sites remain unidentified to-date. Based on the pharmaco-kinetics of the various receptors/binding proteins, CCK_2R can mediate biological effects of only CCK and gastrins, whereas the high-affinity PG binding sites (PG-R?) can mediate biological effects of PGs and gastrins at concentrations measured in the circulation of patients with hypergastrinemia and CRC (reviewed in Rengifo-Cam and Singh, 2004).

In order to understand the cellular mechanisms by which PG and gastrin-like peptides exert growth factor effects on target cells, it is critical that the novel PG/gastrin-binding protein(s) are identified. Thus, the goals of the current study were to identify the high-affinity membrane proteins on the PG/gastrin responsive cell lines, that lack the expression of high-affinity CCK-R, and confirm the functional role of the identified protein(s) in mediating the growth factor effects of PG. Previously, we had identified the presence of $\sim$33–36 kDa gastrin-binding proteins (GBPs) on cellular membranes of colon cancer cells, that were specific for binding gastrin-like peptides, with very low affinity for CCK-like peptides (Chicone *et al*., 1989). In the current study, we improved the methods of crosslinking, solubilization and enrichment of the $\sim$32–36 kDa GBPs, followed by identification by surface-enhanced laser desorption/ionization-time of flight-mass spectrometry (SELDI-TOF-MS) and matrix-assisted laser desorption/ionization-time of flight-mass spectrometry (MALDI-TOF-MS). As a result of these investigations, we discovered that Annexin II (ANX II) represents the high-affinity 32–36 kDa gastrin/PG binding protein. In order to examine the physiological relevance of this unexpected finding, the physical association of ANX II with PG was confirmed *in situ* and *in vitro*. A possible role of ANX II in mediating growth factor effects of PG was determined by downregulating the expression of ANX II using the antisense (AS) strategy. Our studies strongly suggest that membrane-associated ANX II binds PG and gastrins, and partially mediates growth factor effects of these peptides on target cells.

Results

Identification of gastrin responsive cell lines

We and others have previously reported the expression of gastrin gene by human and mouse colon cancer cells (reviewed in Rengifo-Cam and Singh, 2004); data from some of these cell lines can be found in Supplementary material (Supplementary Table 1). Downregulation of gastrin gene expression results in either complete loss, significant loss, slight loss, or no effect on the *in vitro* growth of the cells (Singh *et al*., 1996; Rengifo-Cam and Singh, 2004). These results suggested that whereas some colon cancer cell lines (Colo-320) are extremely dependent on autocrine gastrins for continued proliferation, others were either not dependent (Colo-205A) or variably dependent (CA, HCT-116, DLD-1) (Supplementary Table 1). In the current study, we examined whether these cell lines were responsive to exogenous gastrins, in relation to gastrin gene expression. Representative data from growth assays with one of the cell lines, Colo-320, are presented in Figure 1. PG was relatively more effective than G17 in stimulating the anchorage-dependent (Figure 1a) and anchorage-independent (Figure 1b) growth of Colo-320 cells, especially at 0.1 nM. Essentially similar results were obtained with cancer (CA) cells (data not shown). All other colon cancer cell lines (Supplementary Table 1) were negligibly responsive to exogenous gastrins. In the case of IEC cells, PG was significantly more effective than G17 in stimulating the growth of the cells, especially at lower concentrations, as previously reported (Singh *et al*., 2003).

Results of the growth assays suggested that cell lines expressing significant levels of autocrine gastrins (HCT-116, DLD-1) were generally refractory to the growth effects of exogenously added gastrins (Supplementary Table 1). Surprisingly, however, CA cells in spite of expressing significant levels of autocrine gastrins (Supplementary Table 1) were highly responsive to growth effects of exogenous gastrins, suggesting perhaps that CA cells express high levels of GBPs, thus allowing the cells to respond to both autocrine and exogenous gastrins. In the case of cell lines that expressed negligible to low levels of autocrine gastrins, the cells were either highly responsive (Colo-320), or demonstrated no significant response (Colo-205A, HT-29) (Supplementary Table 1). These results suggest that relative expression of GBPs and autocrine gastrins dictate the response of the cells to exogenously added gastrins. Cell lines that demonstrated a significant response to exogenously added gastrins (Colo-320, CA, IEC-18, Swiss 3T3), irrespective of the level of expression of autocrine gastrins, were selected for further characterization of GBPs.

Expression of CCK_2R and high-affinity binding sites for PG-like peptides (PG-R) on colon cancer cells

None of the human colon cancer cell lines examined by us, including HCT-116 and Colo-320, expressed CCK_2R or CCKC-binding sites, when measured by either reverse transcription–polymerase chain reaction (RT–PCR) or real-time quantitative RT–PCR (Supplementary Figure 1).

On the other hand, we and others have reported the presence of high-affinity gastrin/PG preferring binding sites on a number of cell lines that are responsive to exogenous PG/G17. For example high-affinity

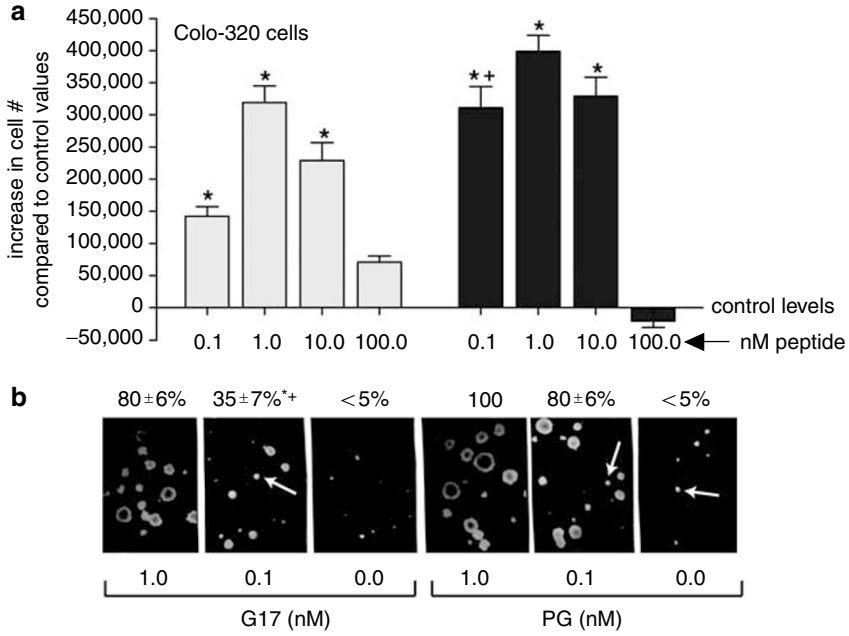

Figure 1 Growth effects of PG and G17 on Colo-320 cells. (**a**) To measure anchorage-dependent growth, $\sim 0.3 \times 10^6$ cells were seeded/35 mm dishes, and at the end of the experiment the no. of cells in the untreated dishes were ~ 0.32–0.37×10^6 cells. The data are presented as an increase in cell numbers in peptide-treated vs control dishes; the cell numbers in control dishes were arbitrarily assigned a zero value. Each bar represents mean ± s.e.m. of six observations from a representative experiment of three similar experiments. $^*P<0.05$ vs control values. $^{\dagger}P<0.05$ vs the corresponding G17 values. (**b**) Anchorage-independent growth of Colo-320 cells. Representative images of colonies growing in agar, in response to the indicated concentrations of the peptides, are presented at $\times 10$ magnification. The number of colonies measured in response to 1.0 nM PG were arbitrarily assigned a 100% value, and the numbers measured in all other dishes are presented as a % of that (as numerically indicated on top of the dishes). *The number of colonies were significantly higher in response to 0.1 nM PG vs 0.1 nM G17 ($P<0.05$, $n=6$); colonies smaller than that indicated by the arrows were not counted. A similar spread of colony sizes were present in the PG vs G17-treated groups for the indicated doses.

($K_d = \sim 1.0$ nM) binding sites for PG are present on IEC and Swiss 3T3 cells, that demonstrate a relative binding affinity (RBA) for gastrins in the order of PG > G17 > CCK8 (Singh *et al*., 1995, 2003). The binding affinity of PG for colon cancer cells was determined by Scatchard analysis, and the RBA of gastrin-like peptides for the PG binding sites determined. Representative data from CA cells are presented in Figure 2. CA cells were positive for 20–30 fmol of high-affinity ($K_d = \sim 1.7$ nM) recombinant human progastrin (rhPG) binding sites/10^6 cells (Figure 2a). The RBA of the gastrin binding sites on CA cells was highest for PG, followed by G17 and appeared to be negligible for CCK-8 (Figure 2b). The binding affinity data from different cell lines are presented in Supplementary Table 2.

Data as presented in Figure 2 and Supplementary Table 2, confirm the presence of high-affinity binding proteins (GBPs) for gastrins on gastrin responsive colon cancer and intestinal/fibroblast cell lines, which were distinct from CCK_2R and the low-affinity CCKC-R. In order to further characterize and identify these novel PG preferring binding proteins/receptors, the molecular mass (M_r) of the proteins was determined.

M_r *of membrane-associated GBPs: effect of crosslinker and pH*

Previously we had used the amino crosslinker, disuccinimidyl suberate (DSS), for crosslinking G2–17 to membrane proteins and reported the presence of ~33, ~45 and ~80 kDa GBPs on normal colonic mucosal membranes (Narayan *et al*., 1992), and the predominant presence of 33–36 kDa proteins on CA tumor membranes (Chicone *et al*., 1989). In the current studies, we further refined the process, and used the carbodiimide crosslinker (EDC) for crosslinking G1–17 to the membrane binding proteins, in the presence or absence of bovine serum albumin (BSA) at pH ranging from 4.5 to 8.0. Representative data with CA tumor membranes are presented in Figure 3a and b. DSS effectively crosslinked ^{125}I-G2–17, but was ineffective with ^{125}I-G1–17 (Figure 3a). EDC effectively crosslinked ^{125}I-G1–17 to all three forms (a, b, c) of GBPs on CA tumors (Figure 3a). The presence or absence of BSA did not significantly affect the relative levels of crosslinked ligand (Figure 3b). Crosslinking of ^{125}I-G17 with EDC to the ~33, ~45 and ~80 kDa membrane binding proteins was most effective at pH 6.0–6.5; at lower pH, specific binding to ~33 and ~45 kDa proteins was either lost or accentuated, respectively (Figure 3b). At pH 7.0 and higher, specific binding to all three bands of proteins was lost (data not shown).

M_r *of GBPs, crosslinked to G1–17 with EDC, before or after solubilization*

Swiss 3T3, Colo-320 and CA tumors were all positive for the three molecular forms of GBPs, arbitrarily

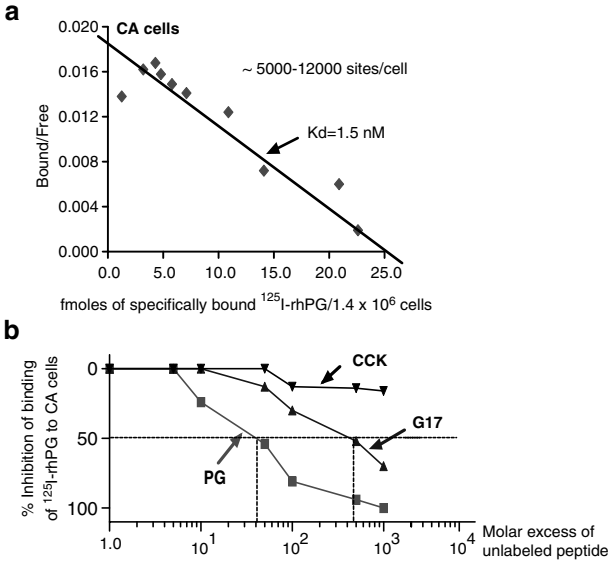

Figure 2 Scatchard plot of specific binding of ^{125}I-rhPG with CA cells (**a**), and RBA of G17 and CCK8 for PG binding sites (**b**). The binding affinity (K_d) and the total number of specific binding sites/cell were determined from the Scatchard plot of specific binding data. A representative Scatchard plot from one of three experiments is presented in panel a. Each data point is mean of duplicate measurements. (**b**) CA cells were incubated with ^{125}I rhPG in the presence or absence of increasing concentrations of either CCK8, G17 or rhPG and RBA calculated. Each point represents the mean values of triplicate measurements from a single experiment, and is representative of three similar experiments. The intraexperimental variation for each data point was <5%. The RBA calculated for each peptide is presented in a tabulated form in Supplementary Table 2.

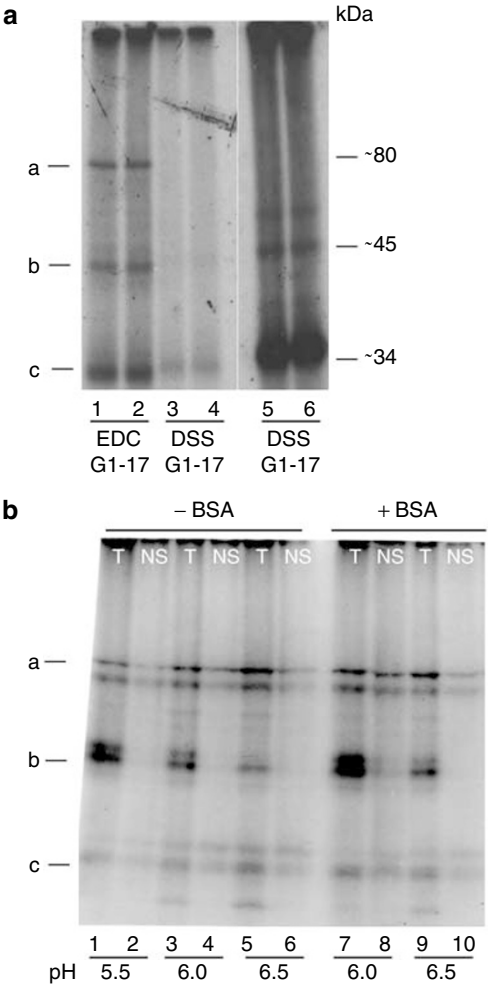

Figure 3 (**a**) M_r of GBPs, crosslinked with DSS or EDC, on tumor membranes. Membranes from CA tumors, labeled with either ^{125}I-G1–17 or ^{125}I-G2–17, and crosslinked with either DSS or EDC were electrophoretically separated. Proteins with M_r of ~34, ~45 and ~80 kDa (a, b, and c bands), bound to ^{125}I-G1–17 were crosslinked with EDC (lanes 1 and 2); DSS poorly crosslinked ^{125}I-G1–17 to GBPs (lanes 3 and 4), but was effective in crosslinking ^{125}I-G2–17 (lanes 5, 6), especially with the 32–36 kDa proteins. (**b**) Effect of pH. Experiments were conducted as described in (**a**), except a wide range of binding buffer pH was used. T = total binding, NS = nonspecific binding. The binding buffers either contained 1% BSA (lanes 7–10) or were devoid of it (lanes 1–6). The three major bands (a, b, and c) of GBPs crosslinked to ^{125}I-G1–17 with EDC, were detected. Binding to proteins in bands b and c was specific whereas binding to proteins in band a was largely nonspecific.

labeled a, b and c (Figure 4). We obtained ~0.5–1.0 mg of membrane proteins from 0.5–1.0 g of tumors. Using the optimally effective detergent buffer (CHAPS and CHS), ~500 μg of proteins were solubilized from 10–20 mg of membrane proteins, resulting in an enrichment of >20-fold upon solubilization of GBPs, and a significant increase in the detection of GBPs in solubilized vs membrane-associated samples (Figure 4a and b). On solubilization, GBPs in bands b and c retained 70–100% specificity for radio-labeled G17, whereas GBPs in band a lost affinity for ^{125}I-G17 (Figure 4a and b), suggesting that the 76–80 kDa GBPs perhaps require association with other membrane protein(s) in order to retain affinity for G17.

The RBA of the solubilized GBPs for binding gastrin-like peptides was examined and representative data from CA cells for bands b and c are presented in Figure 4c. Data from several autoradiographs are presented as bar graphs, demonstrating the % inhibition of binding of ^{125}I-G17 to bands b (Figure 4d) and c (Figure 4e) by the indicated peptides (shown below Figure 4e). Solubilized GBPs in bands b and c demonstrated a relatively high binding affinity for gastrin-like peptides in the order of PG >* GG$\geqslant$G17, with poor affinity for CCK, similar to the data for membrane proteins (Figure 2b, Supplementary Table 2). None of the gastrin-like peptides displaced the binding of ^{125}I-G17 to the solubilized 76 kDa GBPs, but displaced the binding to the 80kDa proteins in band **a** (data not shown). GBPs in band **b** (Figure 4d) appeared to be less discriminatory towards binding the peptides, whereas band **c** proteins appeared to be more discriminatory and demonstrated a preferential binding for PG and GG compared to G17.

The solubilized GBPs were eluted, concentrated and enriched several fold and detected by Coomassie blue on SDS–polyacrylamide gel electrophoresis (SDS–PAGE) gels. Representative data from CA tumors are presented

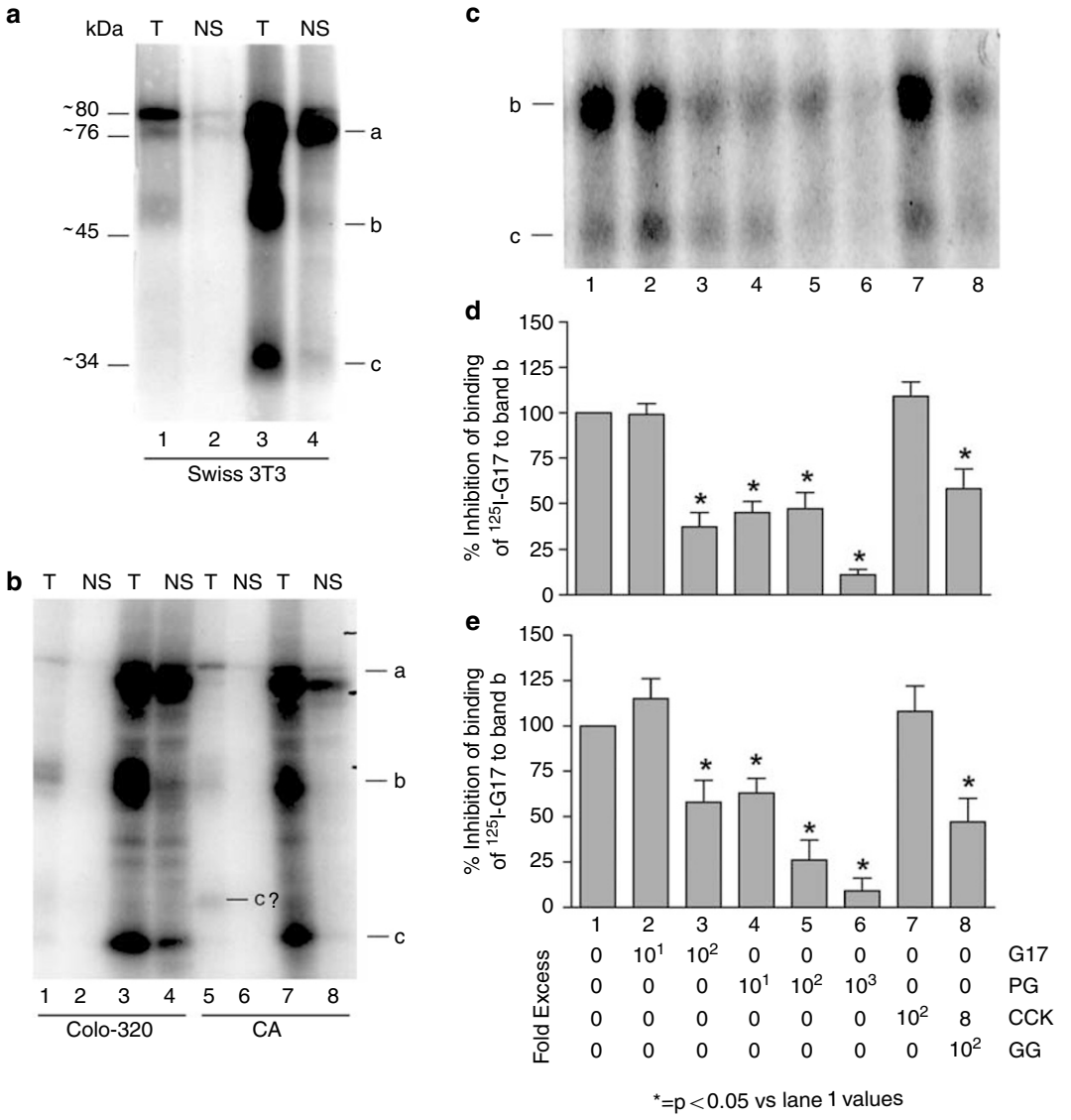

Figure 4 (**a**) and (**b**) Autoradiographs of membrane-associated and solubilized GBPs crosslinked to ^{125}I-G-17. Equivalent protein concentrations (100 μg) from either crude membranes or solubilized membranes were subjected to binding with ^{125}I-G17 in the absence (total binding, T) or presence (nonspecific binding, NS) of 1000-fold excess G17, followed by crosslinking with EDC, and electrophoretic separation. Representative autoradiograms from 1 of 3–10 similar experiments are presented. GBPs on crude membrane proteins from Swiss 3T3 (lanes 1, 2 in **a**), Colo-320 (lanes 1, 2 in **b**) and CA (lanes 5, 6 in **b**) cells are shown. GBPs associated with solubilized membrane proteins from Swiss 3T3 (lanes 3, 4 in **a**), Colo-320 (lanes 3, 4 in **b**) and CA (lanes 7, 8 in **b**) cells are shown. The autoradiograms from IEC cells demonstrated a similar spread of crosslinked bands as measured in Colo-320 cells (data not shown). (**c**–**e**) RBA of solubilized GBPs in bands b and c for PG, GG (Gly extended gastrin), CCK and G17. Solubilized GBPs from CA cells were subjected to binding with ^{125}I G17, in the presence or absence of the indicated concentrations of gastrin-like peptides (legend below panel e), followed by crosslinking with EDC and electrophoretic separation. A representative autoradiogram is presented in (**c**). Data from several autoradiograms from 3–6 experiments are presented as bar graphs for bands b (**d**), and c (**e**). The densitometric reading for bands b and c in lane 1 (total binding) were arbitrarily assigned a 100% value, and readings from lanes 2–8 from all experiments, are presented as a percentage of the lane 1 values in (**d** and **e**), respectively. The fold excess of the competing peptide ranged from 10 (10^1), 100 (10^2) to 1000 (10^3)-fold. Based on the data with 100-fold excess competing peptide, the RBA of GBPs in bands b and c appeared to be in the order of PG > GG > G17 > CCK, which resembled the pattern previously reported for PG-R on IEC cells (Singh *et al*., 2003).

in Figure 5a. The various steps of solubilization, gel elution and concentration resulted in >2000-fold enrichment of GBPs, compared to that present on tumor membranes, resulting in the detection of proteins crosslinked to ^{125}I-G17, as seen from the corresponding autoradiogram (Figure 5a).

Identification of proteins in band c by SELDI-TOF-MS and MALDI-TOF-MS analysis

Proteins in band c (Figure 5a) were arbitrarily divided into two halves (Figure 5b). The information from peptide mapping and database search was definitive from both SELDI and MALDI analysis and identified

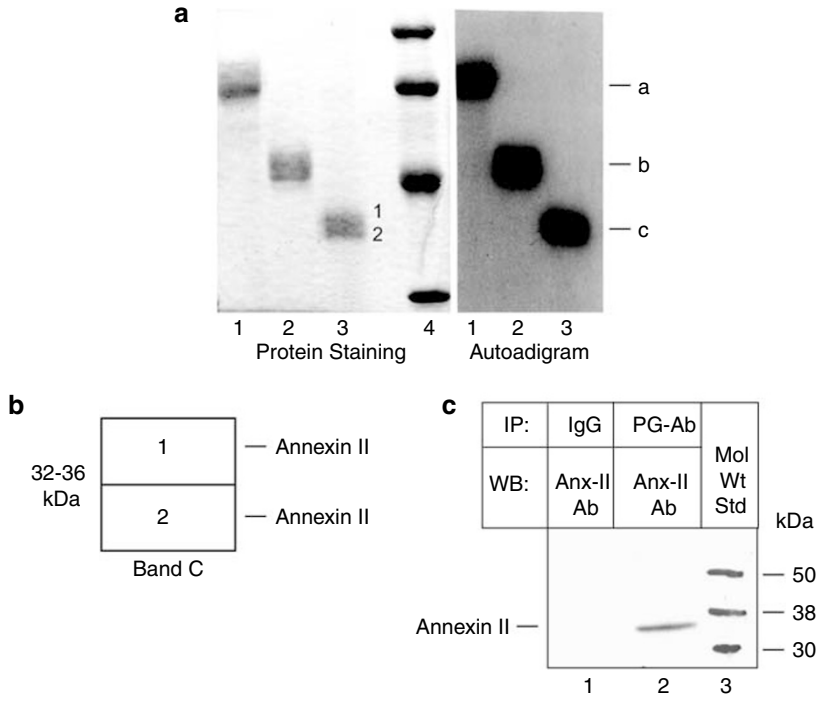

Figure 5 (**a**) Coomassie blue staining and autoradiogram of enriched solubilized GBPs. The solubilized GBPs in bands a, b and c (Figure 4) were enriched several folds and rerun on SDS–PAGE gels. The gels were stained by Coomassie blue and developed autoradiographically. Lane 4 in the left-hand panel represents the molecular weight markers. Lanes 1, 2 and 3 in both the left and right-hand panels represents the enriched proteins in bands a, b, and c, respectively. The concentration of proteins in bands a, b and c was ~500 ng/lane and was obtained from ~1 mg solubilized protein (equivalent to 10–20 mg crude membrane protein). Thus, the yield of GBPs was increased by >1–2K-fold compared to that present on crude membranes. (**b**) Proteins in band c (as shown in Figure 5a) were arbitrarily divided into two equal parts for analysis by SELDI-TOF-MS and MALDI-TOF-MS. Proteins in both halves, 1 and 2, of the 32–36 kDa band c was identified as ANX II. (**c**) Co-IP of ANX II with anti-PG-Abs from HCT-116 cellular lysates. Subconfluent HCT-116 cells were processed for IP with either pre-immune IgG or with anti-PG-Abs (IgG) (lane 2). The IP proteins were processed for WB analysis with anti-ANX II-Abs. Lane 3 = molecular weight standards. The data presented in Figure 5c are representative of three similar experiments.

ANX II in both the halves of band **c**. No other proteins were identified in band c, which appeared to be a homogenous band of ANX II proteins. Identification of ANX II as a possible binding protein (receptor?) for PG-like peptides was unexpected. An interaction of autocrine PG with the monomeric 36 kDa ANX II molecules, *in situ*, was confirmed in pulldown assays with anti-PG-antibodies (Abs) using HCT-116 cellular lysates, followed by Western immunoblot (WB) analysis with anti-ANX II Abs (Figure 5c). The binding of PG with ANX II was further confirmed *in vitro* as described below.

ANX II binds rhPG in solution, in an in vitro *binding assay*

The efficacy of anti-PG-Abs and anti-ANX II-Abs for immunoprecipitating the respective peptide/protein in solution was examined. Both the Abs effectively immunoprecipitated (IP) 60–70% of the respective peptide/protein in solution (Figure 6a and b). In the next set of experiments, rhPG and ANX II were added either separately (lanes 1 and 2 in Figure 6c) or together (lanes 3 and 4 in Figure 6c) in the binding buffer, and IP with either anti-PG-Abs (lane 3, Figure 6c) or anti-ANX II Abs (lane 4, Figure 6c), followed by immunoblot analysis with either anti-PG-Abs (upper panel in Figure 6c) or anti-ANX II Abs (lower panel, Figure 6c). The results provided the first direct evidence that rhPG and ANX II bind in solution and are co-IP by both Abs (Figure 6c). The co-IP rhPG and ANX II were further visualized by Coomassie blue staining (Figure 6d). Surprisingly, rhPG in solution appeared to be unstable and an additional 7 kDa band was evident in lanes 1 and 2 (Figure 6d); the 7kDa band was more evident in lane 2, as the concentration of rhPG was ~10× higher in lane 2 vs lane 1.

RBA of Tenascin-C for binding PG binding sites

ANX II was identified as a receptor protein for tenascin-C (TN-C) (Chung and Erickson, 1994). A splice variant fragment of TN-C, TNfnA-D, had the highest binding affinity for ANX II (Chung and Erickson, 1994). TNfnA-D was therefore obtained from Dr Erickson (Duke University, Durham, NC, USA), and RBA of TNfnA-D for displacing the binding of ^{125}I-PG to representative normal (IEC-18) and CA cells examined. Representative data are presented in Figure 8, and the RBA calculated from several assays are presented in

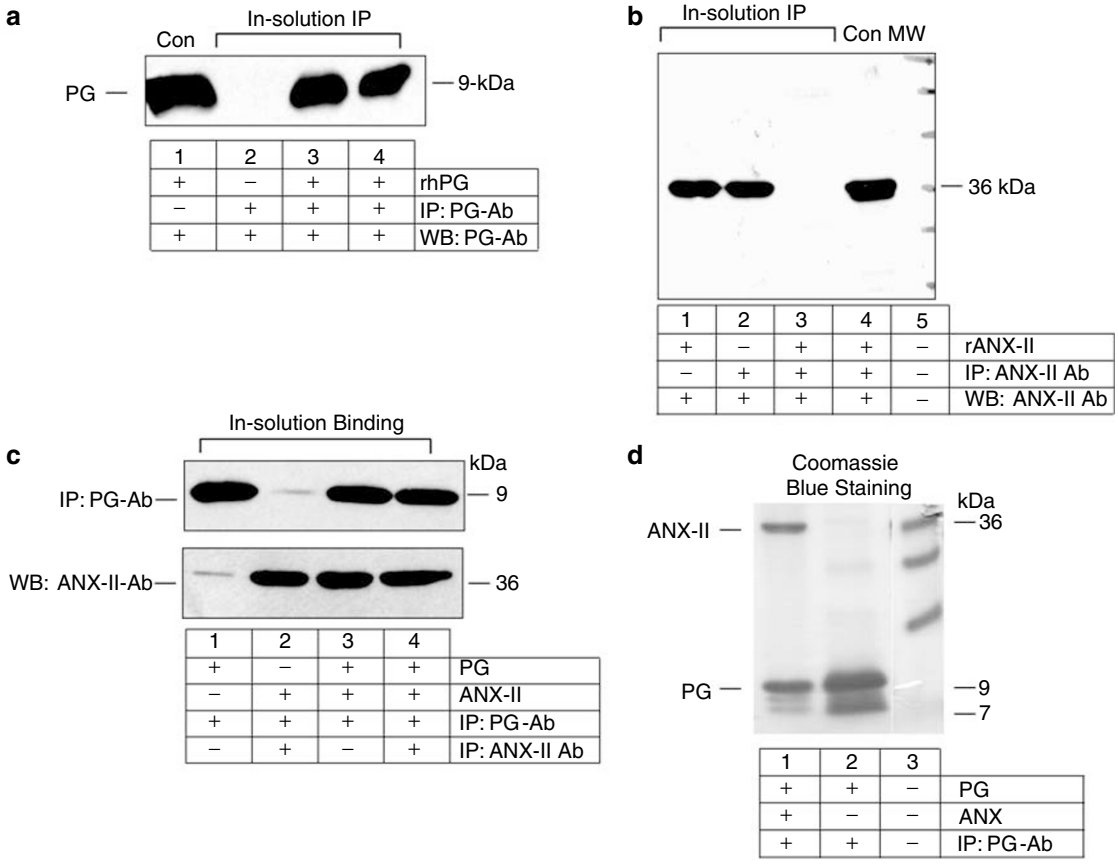

Figure 6 (**a**) and (**b**) Recovery of rhPG and ANX II in solution by IP. rhPG and ANX II (10 μg/lane) were subjected to WB analysis either directly as positive controls (CON) (lane 1 in **a**, lane 4 in **b**), or were IP from the binding assay buffer, using 1:10 dilution of the relevant antibody, followed by WB analysis (lanes 3, 4 in **a**; lanes 1, 2 in **b**). Lanes 1 (**a**) and 4 (**b**) served as positive controls and lanes 2 (**a**) and 3 (**b**) served as negative controls with no peptide added in the solution. The molecular weight markers (MW) are shown in (**b**) in lane 5. In (**a**) the recovery of rhPG from the binding assay solution was determined, using anti-PG-Ab, whereas in (**b**) the recovery of ANX II from solution was analysed using anti-ANX II-Ab. The WB data in (**a** and **b**) is representative of two similar experiments. (**c**) Binding and co-IP of rhPG and ANX II in an *in vitro* binding assay. Binding of rhPG with ANX II in solution, in an *in vitro* binding assay, was examined. In each case, an equal concentration of the two peptides was used ($\sim$0.3 nmol). In lanes 1 and 2, either rhPG or ANX II was added, respectively. In lanes 3 and 4 both rhPG and ANX II were added. Samples in lane 3 were IP with anti-PG-Ab, whereas samples in lane 4 were IP with anti-ANX II–Ab. All the samples were processed for WB with both anti-PG-Ab and anti-ANX II Ab and representative data from one of two separate experiments are presented. (**d**) Coomassie blue staining of samples in lanes 1 and 2 were processed as described above for either lane 3 in (**c**) or lane 3 in (**a**), respectively. Lane 3 = molecular weight markers.

Table 1. The RBA of TN-C for PG binding sites was either slightly higher (Figure 7a, Table 1), or slightly lower (Figure 7b, Table 1), than that of rhPG, suggesting that at least 50–60% of the specific binding sites for rhPG and TN-C are similar on the ANX II molecule. Surprisingly, 40% of the specific binding of PG could not be displaced by even 10 000-fold excess of TN-C, suggesting that $\sim$40% of the PG-binding sites were specific for PG-like peptides, and were not shared with TN-C.

Downregulation of ANX II expression significantly reduces the growth factor effects of PG

Clones of IEC-18 and HCT-116 cells were generated, that either expressed the truncated ANX II protein (S or control clones) or were downregulated for the expression of ANX II (AS clones). The relative expression of ANX II in representative sense (S) and AS clones compared to that in the wild-type IEC-18 cells (C) is presented in Figure 8a. The relative levels of ANX II in C cells were similar that in the S clones, for reasons described in Materials and methods. The AS clones demonstrated a significant loss in the relative expression of ANX II (Figure 8a). A representative IEC-18 clone (AS_2) demonstrated a significant loss ($>70\%$) in its growth response to optimal doses of PG (0.1–1.0 nM), compared to the growth response of S_2 (control) clones (Figure 8b). The growth response of AS_2 and S_2 clones to 1% fetal calf serum (FCS), however, was similar; suggesting that the effects of downregulation of ANX II were specific to PG.

In order to confirm a receptor-like role of ANX II for mediating the growth factor effects of PG, the wild-type (parental) IEC-18 cells were pre-treated with either pre-immune IgG or anti-ANX II-Ab, at two different

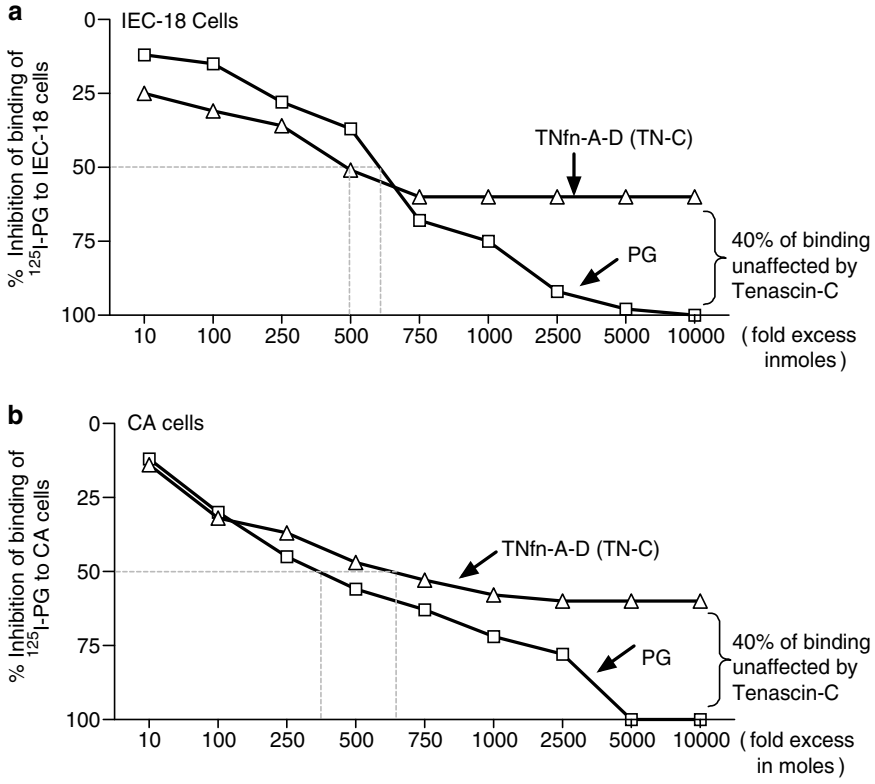

Figure 7 RBA of TNfnA-D for binding PG binding sites. IEC-18 (**a**) and CA (**b**) cells were incubated with ^{125}I rhPG in the presence or absence of increasing concentrations of either TNfnA-D or rhPG. RBA of TNfnA-D for displacing the binding of ^{125}I rhPG to specific PG binding sites (ANX II) on IEC-18 and CA cells was determined from the binding data and is presented in Table 1. Each point in the graph represents a mean value of triplicate measurements from a single experiment, and is representative of two similar experiments. The intraexperimental variation for each data point was $<10\%$. In both cell lines, TNfnA-D only displaced $\sim 60\%$ of the specific binding of ^{125}I rhPG, even at very high concentrations (10 μM).

Table 1 RBA of TNfnA-D (TN-C) for binding PG binding sites

Cells	*PG*	*TN-C*
CA	100%	49 ± 15*
IEC-18	100%	139 ± 21

Abbreviations: CA, cancer; PG, progastrin; RBA, relative binding affinity; TN-C, tenascin-C. *$P<0.05$ vs PG values.

dilutions, followed by measuring the growth response of the cells to either an optimal dose of PG (0.1 nM) or 1% FCS (Figure 8c). The pre-treatment of the cells with the anti-ANX II-Ab (especially at the lower dilution), significantly decreased the growth response of the cells to PG, but not to FCS, providing strong evidence that ANX II may indeed function as a receptor protein for PG/gastrin-like peptides.

A possible role of ANX II in mediating growth effects of autocrine PG was examined in HCT-116 cells. AS-HCT-116 clones were downregulated for the expression of ANX II by $\sim 90\%$ (Figure 9a), confirming a significant sequence homology between rat and human ANX II cDNA. Surprisingly, a few S clones (such as S_7, Figure 9a) demonstrated an increase in the expression of ANX II compared to that measured in non-transfected cells (C), for reasons unknown. As proof of principle, the overexpressing S_7 clone was chosen for the growth studies. As HCT-116 cells express significant levels of autocrine PG and are non-responsive to exogenous PG (Supplementary Table 1), the growth of the clones was measured in response to FCS. FCS dose-dependently increases autocrine expression of gastrin gene (and hence PG), and thus the response to FCS has been used as an indirect means of measuring response to autocrine PG (Singh *et al*., 1996). The growth response of non-transfected (control) HCT-116 cells to increasing concentrations of FCS is shown in Figure 9b. The AS-ANX II-HCT-116 clones demonstrated a significant loss in the growth response by ~ 70–80%, in the presence or absence of FCS (Figure 9c and d). The overexpressing S_7 clones (Figure 9e), demonstrated an enhanced response to FCS, especially at higher concentrations. The relative levels of PG in the cellular lysates of the cells (measured as described previously, Cobb *et al*., 2004) were similar in the S_7, AS_2 and AS_3 clones, compared to that in the C cells (Supplementary Table 3), and increased similarly in all the S, AS and C clones, in a dose-dependent manner, in response to FCS, as published previously (Singh *et al*., 1996); these results suggest that endogenous ANX II likely plays an important role in mediating growth factor effects of autocrine PG.

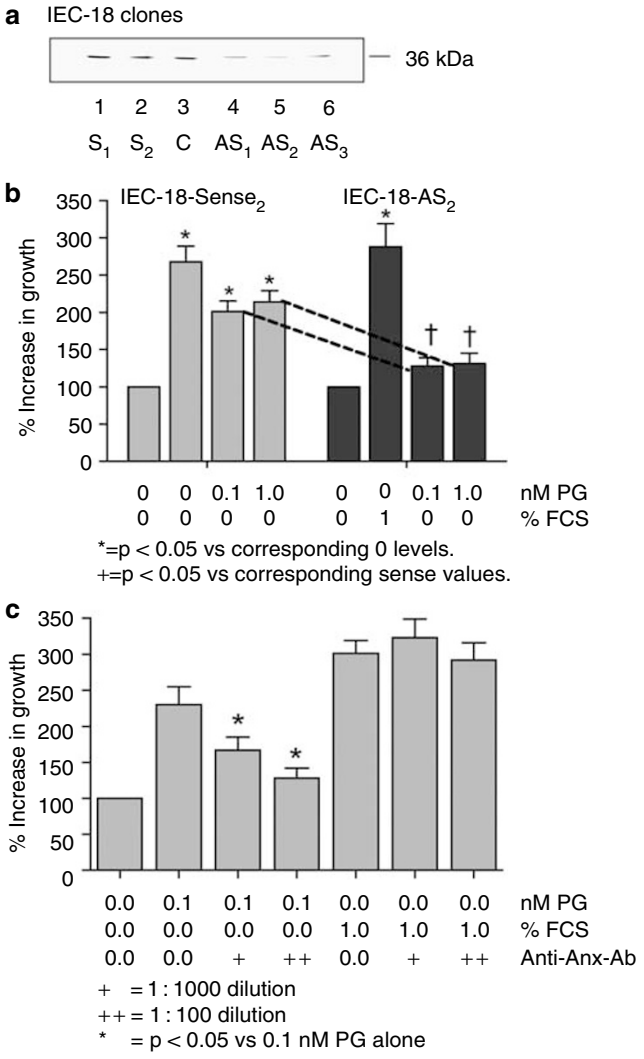

Figure 8 Growth of ANX II-S or ANX II-AS clones of IEC-18 cells in response to rhPG. The S and AS clones of IEC-18 cells were generated. WB data from representative clones are presented in (**a**); wild type (C) cells were not transfected. The S clones, for reasons described in Materials and methods, expressed almost similar levels of ANX II compared to C cells. The AS clones were downregulated for the expression of ANX II by >70%. The total number of specific high-affinity binding sites for PG (measured by a single point assay, as described previously (Singh *et al*., 1995), were significantly reduced by ~65–78% in AS-ANX II clones compared to that in C cells and S clones (data now shown). (**b**) The representative S_2 and AS_2 clones were stimulated to grow in the presence of optimal concentrations of rhPG (0.1, 1.0 nM). FCS (1%) was used as a positive control, and no simulation as a negative control. The growth assays were conducted as described in Methods. Each bar graph represents mean of six observations from a single experiment and is representative of two similar experiments. (**c**) Effect of anti-ANX II-Abs on the growth of IEC-18 cells in response to PG. The parental IEC-18 cells in culture were pretreated with similar concentrations of either anti-ANX II-Abs or pre-immune IgG (control), for 2 h at RT at the indicated dilutions, by our published methods (Singh *et al*., 1994b), followed by the treatment with either 0.1 nM rhPG or 1% FCS as described above. Each bar graph represents mean of four observations from a single experiment and is representative of two similar experiments.

Discussion

In the current studies, we have made the unexpected discovery that the previously reported 33–36 kDa band of GBPs (Chicone *et al*., 1989), represent the multifunctional ANX II protein. This discovery was facilitated by the use of EDC and optimization of detergents, which allowed solubilization of the native binding proteins from cellular membranes. Solubilization of the crosslinked proteins, allowed enrichment of the GBPs and helped us to identify the 33–36 kDa protein as ANX II by SELDI-TOF-MS and MALDI-TOF-MS.

A physical association (binding) of PG with ANX II, *in situ*, was confirmed in HCT-116 cells, known to express autocrine PG (Singh *et al*., 1996). As ANX II associates with cellular membranes, either as a monomer (~33–36 kDa) or as a heterotetramer (AIIt) (two units of S100A or p11 and two units of ANX II; Hajjar and Acharya, 2000), we confirmed that the monomeric 36 kDa ANX II binds PG in an *in vitro* binding assay, strongly suggesting that ANX II can function as a membrane 'receptor' for PG/G17 peptides.

Physiological relevance of binding of ANX II with PG was obtained in experiments with AS-ANX II clones of cells, responsive to either exogenous (IEC-18, Singh *et al*., 2003) or autocrine (HCT-116, Singh *et al*., 1996) PG. Our results suggest that ANX II expression is required for mediating ~50% of the growth effects of exogenous PG on intestinal (IEC) cells. Results with anti-ANX II Abs further confirms a possible important role of ANX II as a receptor-like protein for PG/gastrin-like peptides. Additionally, the growth of AS-ANX II-HCT-116 clones was decreased by >70–80%, and phenocopied the loss of growth of AS-gastrin-HCT-116 clones, as previously reported (Singh *et al*., 1996). These results strongly suggest that the growth factor effects of autocrine PG are attenuated by >80% on downregulation of ANX II expression. The results further highlighted the possibility that ANX II may play a predominant role in mediating growth factor effects of autocrine PG in colon cancer cells, whereas other proteins, besides ANX II, may be required for mediating 100% of the growth factor effects of PG/gastrins on non-tumorigenic (normal) cells such as IEC-18. IP ANX II is a multifunctional protein (Raynal and Pollard, 1994), which binds acid phospholipids and actin with significant affinity (Gerke and Moss, 2002). ANX II is cleaved by chymotrypsin into a 33 kDa C-terminal core domain and a 3 kDa N-terminal domain of 30 amino acids. The first 14 residues of the N-terminal domain contains a high-affinity binding site for S100A10, a Ca^{2+} binding protein (M_r 11K) (Waisman, 1995). Majority of ANX II is tightly associated with p11 forming an ANX $II_2/p11_2$ heterotetramer (AIIt). ANX II is expressed abundantly in rejuvenating cells (fibroblasts, endothelial cells, epithelial cells of the lung and GI tract) (Frohlich *et al*., 1990), and is expressed maximally during S phase and promotes DNA synthesis and cell proliferation (Chiang *et al*., 1993, 1999; Vishwanatha and Kumble, 1993). ANX II expression is increased in many human cancers (Frohlich *et al*.,

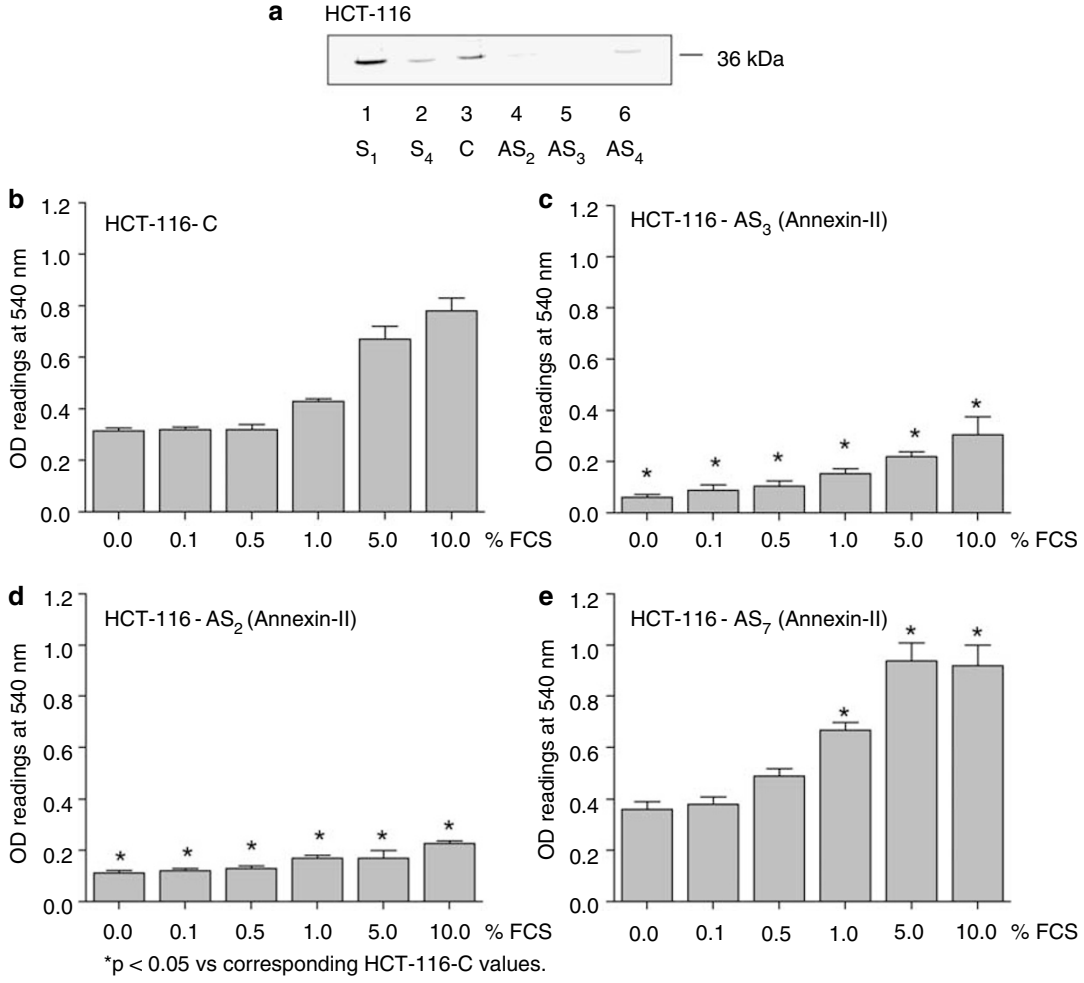

Figure 9 Growth of wild type (C), ANX II-S and ANX II-AS clones of HCT-116 cells, in response to FCS (and hence autocrine PG). S and AS clones of HCT-116 cells were generated. (**a**) Representative WB data from S and AS clones demonstrating relative levels of ANX II expression, compared to that in the control (C) cells is presented. Other than S_7 clones, all other S clones did not overexpress ANX II. All AS clones were significantly downregulated for the expression of ANX II by >80–90%. In previous studies, we have demonstrated that the expression of autocrine PG in HCT-116 cells is increased in a dose-dependent manner in the presence of FCS (Singh *et al*., 1996), as the gastrin gene promoter contains serum response element and is specifically upregulated in the presence of FCS (Rengifo-Cam and Singh, 2004). In the current studies, we confirmed that the relative levels of PG in the AS and S clones increased in a dose-dependent manner in response to increasing concentrations of FCS, similar to that measured in the control cells (Supplemental Table 3). The growth response of the control (HCT-116-C) cells to increasing concentrations of FCS is presented in (**b**). The growth response of two representative AS clones is presented in (**c** and **d**). The growth response of S_7 clone, that was overexpressing ANX II for reasons unknown, is presented in (**e**). Each bar graph represents data from 4–6 observations from a single experiment, and is representative of two similar experiments. * = $P<0.05$ vs corresponding HCT-116-C values.

1990; Vishwanatha *et al*., 1993; Tanaka *et al*., 2004), and downregulation of its expression results in the loss of proliferation (Chiang *et al*., 1999, current studies). All these studies thus strongly suggest that ANX II is a key regulator of DNA synthesis and cell proliferation. High-affinity binding sites for PG (ANX II) are present on colonic and intestinal epithelial cells (Baldwin *et al*., 2001; Singh *et al*., 2003; Rengifo-Cam and Singh, 2004) and colon cancer cells (current studies), but are absent in the brain or liver (unpublished data from our laboratory), which agrees with the reported expression of ANX II (PG 'receptor'), primarily in proliferating cells (Frohlich *et al*., 1990; Chiang *et al*., 1993).

Cellular functions of ANX II are regulated by post-translational modifications and cellular localization. ANX II residues Tyr 23 and Serines 11 and 25 are phosphorylated by c-Src and PKC, respectively (Gould *et al*., 1986), after activation of either insulin receptor (R), or platelet-derived growth factor-R (Brambilla *et al*., 1991; Biener *et al*., 1996). ANX II may thus function as a second messenger for transduction of extracellular signaling pathways. Our current studies suggest that PG/gastrins bind membrane-associated ANX II, which perhaps leads to colocalization and activation of ANX II and c-Src kinase. The latter possibility is highlighted by the fact that PG/gastrins activate c-Src kinase in target cells (Singh *et al*., 1994c; Brown *et al*., 2003; Ferrand *et al*., 2005).

Our studies demonstrate that monomeric ANX II functions as a high-affinity 'receptor' protein for

PG/gastrins. ANX II has previously been described as a high-affinity receptor for the extracellular matrix protein TN-C (Chung and Erickson, 1994), and as a co-receptor on endothelial cells for tissue plasminogen activator, plasminogen and plasmin (Hajjar and Acharya, 2000). AIIt was identified as a receptor for plasmin-induced signaling in human peripheral monocytes, which involved the activation of nuclear factor (NF)-κB, JAK/signal transducers and activators of transcription (STAT) and p38 mitogen-activated protein kinase (MAPK) signaling cascades, leading to a full-scale proinflammatory response (Laumonnier *et al*., 2006). It is possible, that binding of PG to ANX II may mediate an activation of a similar cascade of signaling molecules in target cells, as we and others have reported activation of Src, phosphatidylinositol 3′-kinase/Akt, JAK2, STAT5/3, extracellular signal-regulated kinases, p38 MAPK and NFκB, in response to PG (Hollande *et al*., 2001; Brown *et al*., 2003; Ferrand *et al*., 2005; Rengifo-Cam and Singh, 2005). Importantly, our preliminary findings suggest that treatment of IEC-18 cells with anti-ANX II-Abs results in attenuating the activation of many of the above-described signaling molecules, in response to PG (unpublished data from our laboratory).

At mild acidic pH, AIIt undergoes conformational changes similar to those induced by Ca^{2+}. Thus, ANX II appears to have access to the hydrophobic part of the cellular membranes at both acidic pH in the absence of Ca^{2+} and at neutral pH in the presence of Ca^{2+} (Lambert *et al*., 2004). This may explain our findings of a significant increase in the crosslinking of gastrins to ANX II ($\sim$32–36 kDa) at slightly acidic pH (Figure 3b). The 36 kDa ANX II protein, bound to radio-labeled TNfnA-D, was generally seen as a doublet band in SDS–PAGE (Chung and Erickson, 1994). In freshly prepared membrane extracts, the authors frequently saw a single band of 36 kDa; two lower molecular weight bands appeared at later times (Chung and Erickson, 1994). The authors concluded that as ANX II has two protease cleavage sites near the NH_2 terminus, it likely produces 2–3 closely spaced bands on SDS–PAGE on binding with the ligand such as TN-C (Chung and Erickson, 1994). In the current studies, we also observed the presence of a wide band of 32–36 kDa proteins crosslinked to radio-labeled gastrins (Figure 5), all of which were identified as ANX II by SELDI-TOF-MS. However, in the *in vitro* experiments, in the absence of cell-associated proteases, only a single band of 36 kDa ANX II co-IP with PG (Figure 6).

ANX II expression is upregulated in fibroblasts transformed by v-H-ras, v-src and v-mos (Ozaki and Sakiyama, 1993), and in cells treated with mitogenic or trophic factors such as epidermal growth factor (EGF), fibroblast growth factor, nerve growth factor or transforming growth factor (TGF)-β1 (Keutzer and Hirschhorn, 1990). Upregulation of ANX II was also discovered in gastric epithelial cells infected with *Helicobacter pylori* (Das *et al*., 2005). At the same time, *H. pylori* infection of gastric mucosa, and growth factors such as EGF and TGF-β1 have been reported to increase the expression of gastrin gene, directly or indirectly (Lei *et al*., 2004; Rengifo-Cam and Singh, 2004). These findings suggest the intriguing possibility that the direct (EGF, TGF-β1, oncogenic K-ras) and indirect (*H. pylori*) growth effects of these agents may be magnified by an upregulation of both the gastrin gene (PG) and its binding 'receptor' protein, ANX II.

Overexpression of ANX II and TN-C proteins was measured in a high percentage of CRC, and appeared to correlate with tumor size, depth of invasion and pTNM stage (Emoto *et al*., 2001). Interestingly, treatment of human astrocytoma U373 cells with gastrin resulted in overexpression of TN-C and S100A6 (Kucharczak *et al*., 2001). As c-Jun and NF-κB synergistically transactivate TN-C promoter in primary rat embryo fibroblasts (Mettouchi *et al*., 1997), gastrin may activate TN-C promoter in glioblastoma cells via the same signaling molecules known to be activated in response to PG/gastrins in other cells (Ferrand *et al*., 2005; Rengifo-Cam and Singh, 2005).

Purified ANX II binds TNfnA-D and native TN-C at nanomolar concentrations (Chung and Erickson, 1994).The results of our current studies suggest that PG binds ANX II at the TN-C binding site, either with a significantly higher binding affinity, or equivalent affinity (Figure 7); however, only 60% of the binding sites appear to be common suggesting that either PG binds other proteins besides ANX II or it binds additional binding sites on ANX II that are not displaced by TN-C.

The large TN-C splice variant, containing TNfnA-D, is generally expressed in tissues undergoing active cellular migration or tissue remodeling (Chung and Erickson, 1994). Transformed fibroblasts and fetal lung tissues express TN-C with the A-D domains (Oyama *et al*., 1991). It thus appears likely that the splice variant may facilitate cell migration/invasion and tissue remodeling possibly through binding to ANX II with high affinity (Chung and Erickson, 1994). Based on the literature described above and our current findings, we hypothesize that in the absence of expression of the splice variant form of TN-C, PG likely binds ANX II with a significantly higher binding affinity and dictates the functions of ANX II towards cellular proliferation and progression of the disease. However, on expression of the TN-C splice variant, which may occur during advanced stages of the CRC disease, the splice variant may bind ANX II with equivalent affinity and co-contribute to the functions of ANX II along with PG. Future studies in this field should help to dissect the relative contribution of ANX II, splice variant of TN-C and autocrine PG in the proliferation and metastasis of CRC cells.

Material and methods

Cell culture

Cell lines used in this study include a mouse fibroblast cell line (Swiss 3T3), a normal rat intestinal epithelial cell line (IEC-18), a mouse colon cancer cell line (CA), and human colon cancer

cell lines (Colo-320, HCT-116). The cell lines were obtained and grown as monolayer cultures in the appropriate growth medium, and regularly monitored for the absence of mycoplasma as described previously (Singh *et al*., 1995, 1996, 2003). Stock cultures of cells were subcultured at appropriate intervals to maintain the cells at subconfluent densities. For cell counting and subculturing, the cells were dispersed with 0.05% trypsin and 0.02% ethylene diaminetetraacetic acid (EDTA).

Growth assays

The anchorage-dependent growth assays were conducted as described previously (Singh *et al*., 1995, 1996). Generally, quiescent cells were stimulated with or without various doses of the peptides for 48–72 h in serum-free medium, and the cell numbers measured directly or indirectly in a cell count on an 3-(4,5-dimethylthiazol-2yl)-2,5-diphenyl tetrazolium bromide assay, as described previously (Singh *et al*., 1995, 1996). A soft agar colonogenic assay was conducted for measuring anchorage-independent growth of the cells, as described previously (Singh *et al*., 1996). The total number of colonies/well were counted with the help of an inverted light microscope (Nikon, Houston, TX, USA).

Methods used for RT–PCR analysis of cellular RNA for $hCCK_2R$ and CCKC binding proteins, and real-time quantitative PCR for measuring CCK_2R in human and mouse colon cancer cell lines are provided as Supplementary Method 1.

Binding affinity and RBA of peptides for ^{125}I rhPG binding sites

The full-length recombinant human PG_{1-80} (rhPG) was generated in an *Escherichia coli* expression system and purified and confirmed as described previously (Singh *et al*., 2003). rhPG was radio-labeled with $Na^{125}I$ (Amersham, Chicago, IL, USA), and the intact ^{125}I-rhPG purified by high-pressure liquid chromatography as described previously (Singh *et al*., 2003). For these experiments, cells were expanded *in vitro* in 175 mm flasks and grown to subconfluence in the indicated growth medium containing 10% FCS. All binding assays were performed 36–48 h after seeding the cells in culture medium containing 10% FCS and 2% glutamine. Before the start of the binding assays, the cells in culture were washed with Hanks balanced salt solution (HBSS) (Gibco, Carlsbad, CA, USA) containing 0.1% BSA and 25 mM *N*-2-hydroxyl piperazine-*N*′-2-ehane sulfonic acid (HEPES) (Sigma, St Louis, MO, USA) and scraped with a rubber policeman into conical tissue culture polystyrene tubes. Cells were centrifuged at 500 *g* for 5 min and resuspended in HBSS at a concentration of 2×10^6 cells/ml. Aliquots ($\sim$1.0 ml) of suspended cells in polystyrene tubes were used in the binding assays. Binding assays were conducted as described previously (Singh *et al*., 1995, 2003). For purposes of determining binding affinity, a multipoint (7–12 points) saturation analysis was performed by using increasing concentrations (0.03–1.0 nM) of ^{125}I-rhPG without (total binding) or with (nonspecific binding) 1000-fold excess of radio inert rhPG. The binding data were analysed by a Scatchard plot (Scatchard, 1949). Binding assays were performed at 37°C for 30–60 min at pH 6.5 (optimal for all the cell lines). In order to define the RBA of various peptides for the PG-binding sites on the cells, cells in suspension were incubated with 1.0 nM ^{125}I-rhPG in the presence or absence of increasing concentrations (0.1 nM–10.0 μM) of either the homologous or heterologous peptide. Nonspecific binding was determined in the presence of 1000 $\times$ excess of the non-labeled homologous peptide. At the end of the incubation, the cells were pelleted and washed twice with 1 ml of fresh ice-cold HBSS plus 0.1% BSA. Cell pellets were counted for ^{125}I in a gamma counter with $\sim$70% efficiency for ^{125}I. The RBA of gastrin-like peptides and/or competing peptides for binding the specific binding sites for rhPG were determined from a log-dose inhibition of specific binding of ^{125}I-rhPG by various peptides as described previously (Singh *et al*., 1995, 2003). As reported previously (Singh *et al*., 2003), ^{125}I–rhPG was quite unstable, and therefore all binding assays had to be completed within a day of labeling the peptide.

M_r of GBPs, before or after solubilization

Crude membranes from tumors or cells were used for the determination of M_r of the GBPs as described previously (Chicone *et al*., 1989; Narayan *et al*., 1992). Briefly, in order to prepare crude membranes from tumors, colon cancer cells (CA, Colo-320) and Swiss-3T3 cells were grown in either balb/c mice (CA) or nude mice (Colo-320, Swiss 3T3) as described previously (Singh *et al*., 1987, 1995). The tumors were harvested, and crude membranes prepared from the frozen tumors as described previously (Chicone *et al*., 1989; Narayan *et al*., 1992). Crude membranes were also prepared from cells in culture, by published methods (Singh *et al*., 1995). The crude membranes were then subjected to a binding assay with the indicated radio-labeled gastrin peptide (that were more stable than radio-labeled rhPG), in the presence or absence of 1000-fold excess non-labeled homologous gastrin peptide, as described previously (Chicone *et al*., 1989; Narayan *et al*., 1992; Singh *et al*., 1995). The radio-labeled gastrin peptide bound to the GBPs on the crude membranes was then crosslinked with either the amino crosslinker, DSS (Sigma), as described previously (Chicone *et al*., 1989; Narayan *et al*., 1992; Singh *et al*., 1995), or with the water-soluble EDC as described below. In a few experiments, intact cells in culture were also used as a substrate for crosslinking the radio-labeled peptide to the GBPs on cellular membranes, as described previously (Singh *et al*., 1995). DSS was dissolved in Me_2SO (dimethylsulfoxide (DMSO)), immediately before the use and added to the substrate to give a final concentration of 0.1% DMSO in the HBSS buffer containing phenylmethylsulfonyl fluoride (PMSF), as described previously for Swiss-3T3 cells (Singh *et al*., 1995).

EDC, unlike DSS, catalyses the formation of amide bonds between carboxylic acids and amines to form *O*-acylurea, in the presence of *N*-hydroxysulfosuccinimide ($HOSu[SO_3]$) as a helper reagent (Staros *et al*., 1986). In preliminary studies, we established that 20 mM EDC and 5 mM $HOSu(SO_3)$ were maximally effective for crosslinking the radio-labeled gastrin peptide to crude membranes and intact cells. The major advantage of using EDC as a crosslinker was that the intact radio-labeled gastrin peptide, G17, could be used because the gastrin peptide has several Glu moieties. Additionally, EDC unlike DSS is water soluble and was thus dissolved directly in the binding buffer. Additionally, as DSS is an amino crosslinker, G17, which is blocked at the N-terminus, could not be used and instead radio-labeled G2–17 with a free N-terminus was used. ^{125}I-G1–17 and ^{125}I-G2–17 were prepared and purified as described previously (Chicone *et al*., 1989; Narayan *et al*., 1992; Singh *et al*., 1995). Aliquots of membranes/cells, radio-labeled with the indicated peptide, were either crosslinked with DSS or EDC + HOSu (SO_3), for 15 min at 22°C in the binding buffer containing 1 mM PMSF, in the presence or absence of 1% BSA. The reaction was terminated by rapid centrifugation. The membrane and cellular substrates were washed with excess binding buffer, devoid of BSA, and solubilized by boiling at 100°C for 3–5 min in 0.2 M Tris-HCl buffer, pH 6.8, containing 6% sodium dodecyl sulfate (SDS w/v) 2 mM EDTA, 10% glycerol, v/v, in the presence

of 4% β-mercaptoethanol (v/v). The supernatant was then subjected to SDS–PAGE as described previously (Chicone *et al*., 1989; Narayan *et al*., 1992; Singh *et al*., 1995). The gels were stained, destained, dried and exposed to Kodak XAR-5 film for approximately 7 days at -70°C and the autoradiograms scanned using a laser densitometer.

In order to improve the yield of the crosslinked membrane binding proteins, the native membrane proteins were solubilized with non-ionic and ionic detergents, and the binding of the solubilized proteins with radio-labeled gastrin peptides were examined. In preliminary studies, several detergents were used, including Triton X-100 (Sigma), zwitterionic detergent, 3 [(3-cholamidopropyl)-dimethylammonio]-1-propane sulfonate (CHAPS) (CAL BIOCHEM Logolas, CA, USA), octyl β-glucoside (OBG) and cholesteryl hemisuccinate ester (CHS) (Sigma) by published methods (Ginsberg *et al*., 1978; Gould *et al*., 1981; Naldini *et al*., 1990). Briefly, membranes prepared from tumors/cells (as described above), were reconstituted in HEMGI buffer (20 mM HEPES/KOH (pH 6.8)) containing 5 mM $MgCl_2$, 1 mM ethylene glycol-bis (*b*-aminoethyl ether), 10% glycerol, 0.5% SBTI, Trasylol (Aprotinon) 10 KIU units/ml, 1 mM PMSF and 0.1% bacitracin at a concentration of 15 mg protein/0.5 ml. Various combinations of the detergents (described above) at concentrations ranging from 0.1 to 1% were added to the suspended membrane proteins under ice-cold conditions for 1.5 h at 4°C. The reaction tubes were gently vortexed at 4°C for a few seconds every 10 min. The samples were centrifuged at 15 000 r.p.m. for 45 min at 4°C, and the supernatants containing the solubilized membrane proteins aliquoted in microfuge tubes (1 mg/0.2 ml) and stored at -70°C. The specific binding of the solubilized membrane protein with the radio-labeled ligand was examined by a slight modification of published procedures (Naldini *et al*., 1990). Briefly, aliquots of the solubilized membrane proteins, containing 100–150 μg of protein/tube, were preincubated for 30 min at 4°C in HEMGI buffer containing 0.2% BSA and 5 mM dithiothreitol (DTT, Sigma), in the presence or absence of varying concentrations of the competing peptides. A 1000-fold excess of the homologous peptide was used for defining nonspecific binding. Radio-labeled gastrin peptide was then added to the tubes, and the samples incubated for 30 min at 22°C. The bound radio-labeled gastrin peptide was separated from the unbound peptide by precipitating the bound protein gastrin complex with 0.5 ml of 25% poly (ethylene glycol) + 0.1 ml of bovine γ globulins (5 mg/ml), at room temperature (RT) for 5 min. The precipitate was collected and washed on 0.45 μm cellulose acetate filters (Schleicher and Schuell, Inc., Keene, NH, USA) using a Bio-Rad (Hercules, CA, USA) filter manifold under a vacuum pressure of 25 mm Hg, as described previously (Narayan *et al*., 1992), by published methods (Naldini *et al*., 1990). Radioactivity retained by the filters was determined with a Beckman Gamma 8000 scintillation counter at a counting efficiency of $\sim$70%. As a result of these preliminary studies, a combination of CHAPS and CHS (as described below) was determined to be most effective in solubilizing membrane proteins that retained the highest concentration of specific binding proteins for gastrin-like peptides (data not shown).

The crosslinked membrane preparations were solubilized at a protein concentration of 15 mg/ml with 0.75% (w/v) CHAPS and 0.15% (w/v) CHS (diluted from a 1.25% CHAPS/0.25% CHS (w/v) stock in 20 mM HEPES, pH = 6.5, and 10% glycerol (v/v)), in HEMGI buffer containing the protease inhibitors described above. The reaction mixtures were stirred gently for 1 h at 4°C. The addition of 10% glycerol to the solubilization buffer markedly improved the stability of the solubilized receptor, as published previously (Naldini *et al*., 1990). The reaction mixture was then cleared by ultracentrifugation at 100 000 *g* for 1 h and the supernatant was diluted with HEMGI buffer to a final concentration of 100 μg/0.1 ml, such that the final concentration of CHAPS was reduced to $<$0.2%. The aliquots of solubilized binding proteins, crosslinked to radio-labeled gastrin peptides, were then subjected to SDS–PAGE and autoradiographically developed as described above. In a few experiments, the membranes were subjected to binding with radio-labeled gastrin peptides in the presence or absence of increasing concentrations of the heterologous or homologous peptides, followed by crosslinking and solubilization, in order to determine the RBA of the differentially sized GBPs (separated by SDS–PAGE), for binding gastrin-like peptides.

Elution and enrichment of the crosslinked radio-labeled GBPs

The solubilized membrane proteins, crosslinked with radio-labeled gastrin, were electrophoretically separated and sliced by a gel cutter (Pierce, Rockford, IL, USA) into $\sim$1 mm slices that were placed at the bottom of tubes and counted in a gamma counter. Gel slices associated with peak counts were subjected to protein elution by placing in dialysis tubes containing 1 ml of 0.2 M Tris/acetate (pH 7.4), 1% SDS, 100 mM DTT/0.1 g of wet polyacrylamide gel. The dialysis tubing was dialysed against 50 mM Tris/acetate (pH 7.4), 0.1% SDS, 0.5 mM sodium thioglycolate, for 12–16 h at RT. The gel pieces were then removed from the dialysis tubing, and the tubing further dialysed against several changes of 0.2 M sodium bicarbonate, 0.02% SDS. At the end of the dialysis, the eluted protein within the dialysis tubing was removed and lyophilized. This method allowed us to recover 70–80% of the radioactivity associated with the proteins within the gel slices before dialysis (data not shown).

Eluates from gel slices (representing similarly sized protein bands) from several gels were combined and lyophilized and reconstituted in HMEGI buffer at a concentration of $\sim$1–2 μg/0.2 ml. The reconstituted proteins of different sizes were electrophoretically separated and identified by Coomassie blue staining.

Identification of the 32–36kDa proteins by peptide mapping and database mining

The enriched solubilized proteins, crosslinked to radio-labeled G1–17, were repurified by SDS–PAGE, and visualized by Coomassie blue staining. The protein bands of interest in the 32–36 kDa range were punched out from the gel with a Pasteur pipette into a microfuge tube. An area of the gel with no protein was similarly punched out as a trypsin control whereas one of the molecular weight markers was used as a positive control. The gel pieces in the microfuge tubes were then subjected to destaining with 50% methanol and 10% acetic acid for 1 h at RT $\times$2 with constant shaking, followed by washing with 400 μl of 0.1 M NH_4HCO_3, pH 8.0, for 1 h at RT. The buffer was replaced with 0.5 ml 50% acetonitrile in 0.1 M NH_4HCO_3, pH 8.0 for 1 h at RT. The gel pieces were finally washed with 50 μl of 100% acetonitrile for 15 min at RT, followed by removing all the solvent and drying the gel pieces in a speedvac for about 15 min. The dried gel pieces were finally subjected to digestion with 10 μl of trypsin solution (0.02 μg trypsin/μl in 25 mM NH_4HCO_3, pH 8.0, Promega Corp., Madison, WI, USA). After 15 min of incubation, 20 μl of NH_4HCO_3 buffer was added and the capped tubes incubated for an additional 4 h at 37°C in a dry air incubator. The gel eluates containing the trypsin-digested proteins were then carefully removed and frozen at -80°C until further analysis.

Peptides in the in-gel trypsin digest of band c were detected by SELDI-TOF-MS using the ProteinChip System (Ciphergen Biosystems, Fremont, CA, USA) as described recently (Das *et al*., 2005), with the help of Dr Charlotte Clarke of Ciphergen Biosystems. Peptide masses were searched against the NCBInr database using the ProFound search engine to identify the proteins in the punched out bands of interest. The ProFound is a tool for searching protein sequence databases using information from mass spectral fingerprints. It uses a Bayesian algorithm to rank the protein sequences in the database according to their probability of producing the peptide map. The search output contains the ranked 'hits' (candidate proteins) with their 'coverages' and 'expectation' (*E*) values, based on which the matches can be evaluated. The coverage is the ratio of the protein sequence length covered by the matched peptides. The *E*-value is the number of matches from the database that would be expected to have the same, or a better, score if the matches were completely random. Thus, the lower the *E*-value of a match, the higher the chances that it is a true match. The results obtained by SELDI-TOF-MS were corroborated by MALDI-TOF-MS in the UTMB Biomolecular Resource Facility, with the help of Dr Alex Kurosky, UTMB.

Immunoprecipitation and WB analysis

Cellular lysates were prepared from cells in culture as described previously (Singh *et al*., 1994b; Wu *et al*., 2000, 2003; Cobb *et al*., 2004). Specific Abs generated against rhPG in our laboratory were used (Cobb *et al*., 2004). Mouse monoclonal Abs against ANX II (BD Biosciences, Pharmingen, San Diego, CA, USA) and/or anti-ANX II polyclonal Abs (Santa Cruz, Santa Cruz, CA, USA) were used as per the recommendation of the companies. ANX II-Abs were used for WB analysis of cellular lysates and for immunoprecipitation (IP) of the ANX II complexes by our published methods (Singh *et al*., 1994c; Brown *et al*., 2003). In a few experiments, possible binding/complex formation between rhPG and purified ANX II proteins (Biodesign Intl, Maine, Germany) was examined in an *in vitro* in solution binding assay by published methods (Naldini *et al*., 1990). Briefly, an equimolar concentration of rhPG and ANX II was allowed to bind in a total volume of 50 μl HBSS containing 2 mM $CaCl_2$ at either RT or 37°C. The resulting complexes were analysed by IP. The reaction mixture was diluted two-fold with HBSS buffer and incubated for 1 h with either anti-rhPG-Ab or anti-ANX II-Ab, and then precipitated with protein G Sepharose Beads (Amersham Biosciences, Piscataway, NJ, USA) for 1 h at RT. The beads were washed with HBSS and used for WB analysis with either anti-ANX II- or anti-rhPG-Abs. Appropriate secondary Abs conjugated to horseradish peroxidase were used and the antigen–antibody complexes were detected with the help of ECL + (Amersham Pharmacia Biotech, Piscataway, NJ, USA), as described previously (Singh *et al*., 1994c; Brown *et al*., 2003).

Generation of S and AS ANX II RNA-expressing clones of HCT-116 and IEC-18 cells

The mammalian expression vectors (pCDNA I), containing human ANX II cDNA (9–970 bp) in either the S or the AS orientation, were obtained from Dr JK Vishwanatha (Chiang *et al*., 1999). The S and AS vectors were further amplified and confirmed in the recombinant Molecular Biology Core Facility at UTMB. The ANX II cDNA used in the constructs had a deletion of the first 9 base pairs, and hence was not expected to overexpress ANX II (Chiang *et al*., 1999). The expression of the S and As cDNA was under the transcriptional control of CMV promoter (Chiang *et al*., 1999). The S and AS vectors were used for generating the S (control) and AS clones of HCT-116 and IEC-18 cells by our published methods (Singh *et al*., 1994a, 1996). The S and AS clones of the cell lines thus generated were confirmed by WB analysis with anti-ANX II-Abs and maintained under drug selection pressure using G418, as described previously (Singh *et al*., 1994a, 1996).

Abbreviations

Abs, antibodies; ANX II, Annexin II; BSA, bovine serum albumin; CCK_2R, cholecystokinin type 2 receptor; CCK, choecystokinin octapeptide; CRC, colorectal cancer; DSS, disuccinimidyl suberate; EDC, carbodiimide crosslinker G17, gastrin 1–17; MALDI-TOF-MS, matrix-assisted laser desorption/ionization-time of flight-mass spectrometry; M_r, molecular mass; rhPG, recombinant human progastrin; SELDI-TOF-MS, surface-enhanced laser desorption/ionization-time of flight-mass spectrometry.

Acknowledgements

This work was supported by Grant #s CA097959 and CA72992 from the National Cancer Institute to P Singh.

References

Aly A, Shulkes A, Baldwin GS. (2001). Short term infusion of glycine-extended gastrin(17) stimulates both proliferation and formation of aberrant crypt foci in rat colonic mucosa. *Int J Cancer* **94**: 307–313.

Baldwin GS, Hollande F, Yang Z, Karelina Y, Paterson A, Strang R *et al*. (2001). Biologically active recombinant human progastrin(6–80) contains a tightly bound calcium ion. *J Biol Chem* **276**: 7791–7796.

Biener Y, Feinstein R, Mayak M, Kaburagi Y, Kadowaki T, Zick Y. (1996). Annexin II is a novel player in insulin signal transduction. Possible association between annexin II phosphorylation and insulin receptor internalization. *J Biol Chem* **271**: 29489–29496.

Brambilla R, Zippel R, Sturani E, Morello L, Peres A, Alberghina L. (1991). Characterization of the tyrosine phosphorylation of calpactin I (annexin II) induced by platelet-derived growth factor. *Biochem J* **278**(Part 2): 447–452.

Brown D, Yallampalli U, Owlia A, Singh P. (2003). pp60c-Src Kinase mediates growth effects of the full-length precursor progastrin1-80 peptide on rat intestinal epithelial cells, *in vitro*. *Endocrinology* **144**: 201–211.

Chakladar A, Dubeykovskiy A, Wojtukiewicz LJ, Pratap J, Lei S, Wang TC. (2005). Synergistic activation of the murine gastrin promoter by oncogenic Ras and beta-catenin involves SMAD recruitment. *Biochem Biophys Res Commun* **336**: 190–196.

Chiang Y, Rizzino A, Sibenaller ZA, Wold MS, Vishwanatha JK. (1999). Specific down-regulation of annexin II expression in human cells interferes with cell proliferation. *Mol Cell Biochem* **199**: 139–147.

Chiang Y, Schneiderman MH, Vishwanatha JK. (1993). Annexin II expression is regulated during mammalian cell cycle. *Cancer Res* **53**: 6017–6021.

Chicone L, Narayan S, Townsend Jr CM, Singh P. (1989). The presence of a 33–40 KDa gastrin binding protein on human and mouse colon cancer. *Biochem Biophys Res Commun* **164**: 512–519.

Chung CY, Erickson HP. (1994). Cell surface annexin II is a high affinity receptor for the alternatively spliced segment of tenascin-C. *J Cell Biol* **126**: 539–548.

Cobb S, Wood T, Ceci J, Varro A, Velasco M, Singh P. (2004). Intestinal expression of mutant and wild-type progastrin significantly increases colon carcinogenesis in response to azoxymethane in transgenic mice. *Cancer* **100**: 1311–1323.

Das S, Sierra JC, Soman KV, Suarez G, Mohammad AA, Dang TA *et al*. (2005). Differential protein expression profiles of gastric epithelial cells following Helicobacter pylori infection using ProteinChips. *J Proteome Res* **4**: 920–930.

Dockray GJ, Varro A, Dimaline R. (1996). Gastric endocrine cells: gene expression, processing, and targeting of active products. *Physiol Rev* **76**: 767–798.

Emoto K, Yamada Y, Sawada H, Fujimoto H, Ueno M, Takayama T *et al*. (2001). Annexin II overexpression correlates with stromal tenascin-C overexpression: a prognostic marker in colorectal carcinoma. *Cancer* **92**: 1419–1426.

Ferrand A, Bertrand C, Portolan G, Cui G, Carlson J, Pradayrol L *et al*. (2005). Signaling pathways associated with colonic mucosa hyperproliferation in mice overexpressing gastrin precursors. *Cancer Res* **65**: 2770–2777.

Frohlich M, Motte P, Galvin K, Takahashi H, Wands J, Ozturk M. (1990). Enhanced expression of the protein kinase substrate p36 in human hepatocellular carcinoma. *Mol Cell Biol* **10**: 3216–3223.

Gerke V, Moss SE. (2002). Annexins: from structure to function. *Physiol Rev* **82**: 331–371.

Ginsberg BH, Cohen RM, Kahn CR, Roth J. (1978). Properties and partial purification of the detergent-solubilized insulin receptor: a demonstration of negative cooperativity in micellar solution. *Biochim Biophys Acta* **542**: 88–100.

Gould KL, Woodgett JR, Isacke CM, Hunter T. (1986). The protein-tyrosine kinase substrate p36 is also a substrate for protein kinase C *in vitro* and *in vivo*. *Mol Cell Biol* **6**: 2738–2744.

Gould RJ, Ginsberg BH, Spector AA. (1981). Effects of octyl beta-glucoside on insulin binding to solubilized membrane receptors. *Biochemistry* **20**: 6776–6781.

Hajjar KA, Acharya SS. (2000). Annexin II and regulation of cell surface fibrinolysis. *Ann NY Acad Sci* **902**: 265–271.

Hollande F, Choquet A, Blanc EM, Lee DJ, Bali JP, Baldwin GS. (2001). Involvement of phosphatidylinositol 3-kinase and mitogen-activated protein kinases in glycine-extended gastrin-induced dissociation and migration of gastric epithelial cells. *J Biol Chem* **276**: 40402–40410.

Hollande F, Imdahl A, Mantamadiotis T, Ciccotosto GD, Shulkes A, Baldwin GS. (1997). Glycine-extended gastrin acts as an autocrine growth factor in a nontransformed colon cell line. *Gastroenterology* **113**: 1576–1588.

Keutzer JC, Hirschhorn RR. (1990). The growth-regulated gene 1B6 is identified as the heavy chain of calpactin I. *Exp Cell Res* **188**: 153–159.

Koh TJ, Dockray GJ, Varro A, Cahill RJ, Dangler CA, Fox JG *et al*. (1999). Overexpression of glycine-extended gastrin in transgenic mice results in increased colonic proliferation. *J Clin Invest* **103**: 1119–1126.

Kopin AS, Lee YM, McBride EW, Miller LJ, Lu M, Lin HY *et al*. (1992). Expression cloning and characterization of the canine parietal cell gastrin receptor. *Proc Natl Acad Sci USA* **89**: 3605–3609.

Kucharczak J, Pannequin J, Camby I, Decaestecker C, Kiss R, Martinez J. (2001). Gastrin induces over-expression of genes involved in human U373 glioblastoma cell migration. *Oncogene* **20**: 7021–7028.

Lambert O, Cavusoglu N, Gallay J, Vincent M, Rigaud JL, Henry JP *et al*. (2004). Novel organization and properties of annexin 2-membrane complexes. *J Biol Chem* **279**: 10872–10882.

Laumonnier Y, Syrovets T, Burysek L, Simmet T. (2006). Identification of the annexin A2 heterotetramer as a receptor for the plasmin-induced signaling in human peripheral monocytes. *Blood* **107**: 3342–3349.

Lei S, Dubeykovskiy A, Chakladar A, Wojtukiewicz L, Wang TC. (2004). The murine gastrin promoter is synergistically activated by transforming growth factor-beta/Smad and Wnt signaling pathways. *J Biol Chem* **279**: 42492–42502.

Mettouchi A, Cabon F, Montreau N, Dejong V, Vernier P, Gherzi R *et al*. (1997). The c-Jun-induced transformation process involves complex regulation of tenascin-C expression. *Mol Cell Biol* **17**: 3202–3209.

Naldini L, Cirillo D, Moody TW, Comoglio PM, Schlessinger J, Kris R. (1990). Solubilization of the receptor for the neuropeptide gastrin-releasing peptide (bombesin) with functional ligand binding properties. *Biochemistry* **29**: 5153–5160.

Narayan S, Chicione L, Singh P. (1992). Characterization of gastrin binding to colonic mucosal membranes of guinea pigs. *Mol Cell Biochem* **112**: 163–171.

Ottewell PD, Varro A, Dockray GJ, Kirton CM, Watson AJ, Wang TC *et al*. (2005). COOH-terminal 26-amino acid residues of progastrin are sufficient for stimulation of mitosis in murine colonic epithelium *in vivo*. *Am J Physiol Gastrointest Liver Physiol* **288**: G541–G549.

Oyama F, Hirohashi S, Shimosato Y, Titani K, Sekiguchi K. (1991). COOH-terminal 26-amino acid residues of progastrin are sufficient for stimulation of mitosis in murine colonic epithelium *in vivo*. *Cancer Res* **51**: 4876–4881.

Ozaki T, Sakiyama S. (1993). Molecular cloning of rat calpactin I heavy-chain cDNA whose expression is induced in v-src-transformed rat culture cell lines. *Oncogene* **8**: 1707–1710.

Raynal P, Pollard HB. (1994). Annexins: the problem of assessing the biological role for a gene family of multifunctional calcium- and phospholipid-binding proteins. *Biochim Biophys Acta* **1197**: 63–93.

Rengifo-Cam W, Singh P. (2004). Role of progastrins and gastrins and their receptors in GI and pancreatic cancers: targets for treatment. *Curr Pharm Des* **10**: 2345–2358.

Rengifo-Cam W, Singh P. (2005). Anti-apoptotic effects of progastrins are mediated by NfkP65 activation in AR42J pancreatic cancer cells. *Gastroenterology* **128**: A485.

Scatchard G. (1949). The attraction of protiens for small molecules and ions. *Ann NY Acad Sci* **51**: 660–672.

Seva C, Dickinson CJ, Yamada T. (1994). Growth-promoting effects of glycine-extended progastrin. *Science* **265**: 410–412.

Siddheshwar RK, Gray JC, Kelly SB. (2001). Plasma levels of progastrin but not amidated gastrin or glycine extended gastrin are elevated in patients with colorectal carcinoma. *Gut* **48**: 47–52.

Singh P, Dai B, Dhruva B, Widen SG. (1994a). Episomal expression of sense and antisense insulin-like growth factor (IGF)-binding protein-4 complementary DNA alters the

mitogenic response of a human colon cancer cell line (HT-29) by mechanisms that are independent of and dependent upon IGF-I. *Cancer Res* **54**: 6563–6570.

Singh P, Dai B, Yallampalli C, Xu Z. (1994b). Expression of IGF-II and IGF-binding proteins by colon cancer cells in relation to growth response to IGFs. *Am J Physiol* **267**: G608–G617.

Singh P, Le S, Beauchamp RD, Townsend Jr CM, Thompson JC. (1987). Inhibition of pentagastrin-stimulated up-regulation of gastrin receptors and growth of mouse colon tumor in vivo by proglumide, a gastrin receptor antagonist. *Cancer Res* **47**: 5000–5004.

Singh P, Lu X, Cobb S, Miller BT, Tarasova N, Varro A *et al*. (2003). Progastrin1-80 stimulates growth of intestinal epithelial cells *in vitro* via high-affinity binding sites. *Am J Physiol Gastrointest Liver Physiol* **284**: G328–G339.

Singh P, Narayan S, Adiga RB. (1994c). Phosphorylation of pp62 and pp54 src-like proteins in a rat intestinal cell line in response to gastrin. *Am J Physiol* **267**(2 Part 1): G235–G244.

Singh P, Owlia A, Espeijo R, Dai B. (1995). Novel gastrin receptors mediate mitogenic effects of gastrin and processing intermediates of gastrin on Swiss 3T3 fibroblasts. Absence of detectable cholecystokinin (CCK)-A and CCK-B receptors. *J Biol Chem* **270**: 8429–8438.

Singh P, Owlia A, Varro A, Dai B, Rajaraman S, Wood T. (1996). Gastrin gene expression is required for the proliferation and tumorigenicity of human colon cancer cells. *Cancer Res* **56**: 4111–4115.

Singh P, Velasco M, Given R, Varro A, Wang TC. (2000a). Progastrin expression predisposes mice to colon carcinomas and adenomas in response to a chemical carcinogen. *Gastroenterology* **119**: 162–171.

Singh P, Velasco M, Given R, Wargovich M, Varro A, Wang TC. (2000b). Mice overexpressing progastrin are predisposed for developing aberrant colonic crypt foci in response to AOM. *Am J Physiol Gastrointest Liver Physiol* **278**: G390–G399.

Staros JV, Wright RW, Swingle DM. (1986). Enhancement by N-hydroxysulfosuccinimide of water-soluble carbodiimide-mediated coupling reactions. *Anal Biochem* **156**: 220–222.

Tanaka T, Akatsuka S, Ozeki M, Shirase T, Hiai H, Toyokuni S. (2004). Redox regulation of annexin 2 and its implications for oxidative stress-induced renal carcinogenesis and metastasis. *Oncogene* **23**: 3980–3989.

Vishwanatha JK, Chiang Y, Kumble KD, Hollingsworth MA, Pour PM. (1993). Enhanced expression of annexin II in human pancreatic carcinoma cells and primary pancreatic cancers. *Carcinogenesis* **14**: 2575–2579.

Vishwanatha JK, Kumble S. (1993). Involvement of annexin II in DNA replication: evidence from cell-free extracts of Xenopus eggs. *J Cell Sci* **105**(Part 2): 533–540.

Waisman DM. (1995). Annexin II tetramer: structure and function. *Mol Cell Biochem* **149–150**: 301–322.

Wang TC, Koh TJ, Varro A, Cahill RJ, Dangler CA, Fox JG *et al*. (1996). Processing and proliferative effects of human progastrin in transgenic mice. *J Clin Invest* **98**: 1918–1929.

Wank SA, Pisegna JR, DE Weerth A. (1992). Brain and gastrointestinal cholecystokinin receptor family: structure and functional expression. *Proc Natl Acad Sci USA* **89**: 8691–8695.

Wu H, Owlia A, Singh P. (2003). Precursor peptide progastrin(1-80) reduces apoptosis of intestinal epithelial cells and upregulates cytochrome c oxidase Vb levels and synthesis of ATP. *Am J Physiol Gastrointest Liver Physiol* **285**: G1097–G1110.

Wu H, Rao GN, Dai B, Singh P. (2000). Autocrine gastrins in colon cancer cells Up-regulate cytochrome c oxidase Vb and down-regulate efflux of cytochrome c and activation of caspase-3. *J Biol Chem* **275**: 32491–32498.

Zhang QX, Baldwin GS. (1994). Structures of the human cDNA and gene encoding the 78 kDa gastrin-binding protein and of a related pseudogene. *Biochim Biophys Acta* **1219**: 567–575.

Supplementary Information accompanies the paper on the Oncogene website (http://www.nature.com/onc).